OA-1 315

MILITARY TECHNICAL COLLEGE

CAIRO - EGYPT

NORMAL PERFORATION OF THIN DURALUMIN PLATES AT ORDNANCE VELOCITIES

A.M.Riad*, H.Yakout**, M.S.Abdel-Kader**, and Y.Kresha***

ABSTRACT

This paper describes an experimental investigation of ballistic perforation of thin duralumin plates struck by the standard 7.62 mm bullet. It also simulates experimentally obtained results using Ravid-Bodner two-dimensional analytical model (1983) for plates exhibiting plugging failure. Five impact velocities ranging from 220 to 700 m/s and plates of 1.6, 3 and 4 mm thickness are considered. The plates mechanical properties are also changed by a heat treatment procedure which consists of solution hardening followed by artificial ageing.

It is found that the changes in projectile velocity drop and in its energy loss with impact velocity are qualitatively similar. It is also found that the penetration resistance of treated plates is generally greater than the as-received ones, although the former have smaller yield and ultimate strengths. The specific energy loss increases with the increase of plate thickness for the as-received duralumin plates, while it first decreases and then increases for the treated plates. Predicted responses employing the five-stage analytical model of Ravid and Bodner are also obtained and compared with experimentally obtained responses. Good agreement is generally obtained.

* Teaching Asst., ** Asst. Prof., *** Associate Prof., Dept. of Weapons and Ammunition, M.T.C., Cairo, EGYPT.

INTRODUCTION

"Penetration" is essentially a mutual interaction between the projectile and the target. The process is affected by numerous parameters (cf. Refs. [1,2] and Fig.1). These parameters are divided into : (i) impact conditions, (ii) projectile characteristics, and (iii) target characteristics. Because of the great variety of possible interactions between these parameters, the target may fail by different mechanisms, the most important of which are shown in Fig. 2. These include petalling, ductile hole enlargement, plugging, and fragmentation. Such failure modes may be operative either individually or in combination [3].

Efforts have been recently directed towards developing sound quasi-analytical and analytical models to simulate and/or predict experimental responses of thin target plates subjected to penetration. These models are based on energy balance and/or momentum conservation, along with certain simplifying assumptions [4,5].

The Ravid-Bodner analytical model [5] is chosen in the present work to model the perforation of thin duralumin plates. This model is based on the energy balance principle and takes into consideration the influence of material strain-rate dependence on its dynamic behaviour. The model describes the process in five distinct but interconnected stages. The input data to the model are simple geometrical dimensions and some experimental data which are easily determined. The output of this model includes the projectile and plug velocities as well as the time histories of resisting force, projectile velocity and its displacement. A complete formulation of the Ravid-Bodner model is presented and compiled into a FORTRAN computer program.

This paper is concerned with an experimental investigation of the effect of projectile impact velocity, plate thickness and target mechanical properties on the penetration process. Also, comparison of predicted responses based on the Ravid-Bodner model and experimental results confined to plates exhibiting plugging failure is performed.

EXPERIMENTAL PROCEDURE

The experimental work consists of the following phases : (i) material characterization, (ii) ballistic tests, and (iii) post-firing examinations. The characterization of the as-received duralumin plates consisted of performing chemical analysis, as well as measuring hardness, tensile strength, and strain to fracture (ductility). The chemical analysis of duralumin was done on a direct reading emmission spectrometer (Model POLYVAC-E982). A Brinell hardness test was performed by application of a load of 312.5 N on a 2.5 mm steel ball in contact with prepared specimen. The quasi-static tensile tests were performed on a tensile/compressive testing machine (Model AWPMA). The engineering stress-strain curves were deduced from the autographically recorded load-displacement curves, then the values of yield and ultimate tensile strengths as well as strain to fracture were obtained.

The mechanical properties of some as-received plates were changed by a heat treatment cycle consisting of solution hardening followed by artificial ageing, as shown in Fig.3. The mechanical properties of the treated duralumin plates were then measured.

The ballistic experiments were performed to measure the projectile shape coefficient, its impact and post-perforation velocities, as well as time of penetration for different target plates. The ballistic set-up consists of 7.62 mm ballistic rifle, impact and post-perforation velocities frames, target plate mount, projectile stopping arrangement, splinters trapper and universal electronic counters (EC). A schematic of the ballistic set-up is shown in Fig.4.

The shape coefficient of the 7.62 mm standard projectile is determined in ballistic shooting range by measuring its velocity at two points along its trajectory (V_1 and V_2) separated by a distance L. Based on the principle of energy conservation, the projectile shape coefficient, i, can be determined by the following equation [6] :

$$i = \frac{4m}{\rho A_p C_x(\bar{V}/a)} \frac{(V_2 - V_1)}{(V_2 + V_1)} \frac{1}{L}, \qquad (1)$$

where m is the projectile mass, ρ is the air specific mass, A_p is the projectile cross-sectional area, $C_x(\bar{V}/a)$ is the function of air resistance, $\bar{V}$ is the mean velocity ($\triangleq[V_1+V_2]/2$), and a is the sound velocity in air.

The projectile velocity was indirectly determined by measuring time of its flight over a fixed distance (reference base). Projectile arrival at the pre-determined base ends was detected by connection of electric circuits. The amount of powder charge was changed to vary the projectile impact velocity. Five charges (0.5, 0.8, 1.1, 1.4 and 1.6 grams) were prepared to provide impact velocities ranging from 220 to 700 m/s. The number of fired shots n for each charge used was 35 ± 2. The average impact velocity $\bar{V}$ and the coressponding confidence interval $\pm \Delta\bar{V}$ (based on 95.5% probability of success) were calculated using the following equations [7,8] :

$$\bar{V} = \sum_{i=1}^{n} \frac{V_{xi}}{n} \pm \frac{id^2}{m} \times 10^3 \frac{\Delta x}{[dD(V)/dV]_{\bar{V}_x}}, \qquad (2)$$

$$\Delta\bar{V} = \pm \frac{t_{\alpha,n-1}}{\sqrt{n}} \sigma \quad , \qquad (3)$$

where V_{xi} is the measured velocity at distance x from the muzzle for shot i, d is the weapon calibre, Δx is the distance from the reference base midpoint to the required point, m is the projectile mass, $[dD(V)/dV]_{\bar{V}_x}$ is the derivative of the function of air resistance, $t_{\alpha,n-1}$ is a function of confidence level α and degrees of freedom $n-1$, and σ is the group standard deviation.

The mean post-perforation velocity was evaluated for each charge by recording a minimum of 5 measurements for each target plate. Some recorded shots were rejected using Chauvent's criterion [7], then the average velocity and the corresponding confidence interval were evaluated using Eqs. (2) and (3).

The penetration time of as-received duralumin plates was measured by using two frames. The first frame was located in front of the target, while the second one was put behind it. The penetration time (Δt) is :

$$\Delta t = t_2 - t_1 , \qquad (4)$$

where t_1 is the projectile travel time measured with the target removed, and t_2 is the time when the target is in place.

Post-firing examinations of target plates were performed in order to study the type of failure the plates had undertaken and the geometry and characteristics of the perforation and the ejected plug. This included the measurements of the petals height and number in case of petalling, as well as the perforation diameter, mass and dimensions of plug in case of plugging. The input diameter of the perforation hole was also measured. All interesting features related to target failure mode, plugs and projectiles were photographed for later use in the analysis of test results. A detailed discussion of the experimental procedure is available in Chapter 3 of Ref. [1].

EXPERIMENTAL RESULTS AND DISCUSSIONS

This section presents experimentally obtained results together with relevant analyses and discussions. The results are classified into material characterization, ballistic firing test results, and post-firing examinations of as-received and treated duralumin target plates within the chosen ranges of plate thickness and projectile impact velocity.

Material Characterization Results

The chemical analysis of the available duralumin plates has shown that the plates had almost the same chemical composition; Table 1 presents an average result. The hardness test results have shown that the as-received plates had a hardness of 1100 ± 100 MPa, while the treated ones had a hardness of 1000 ± 100 MPa. Representative load-displacement curves which were recorded during the quasi-static tensile tests of the as-received plates are shown in Fig.5. The average engineering stress-strain curves for duralumin plates are deduced from the load-displacement curves. The average values of plate hardness, yield strength, ultimate strength, and strain to fracture are shown in Fig. 6 for the as-received and treated plates. It is clear that the treated plates have lower yield and ultimate strengths and higher ductility than the as-received ones.

Ballistic Test Results

Four to five shots were fired for each charge in order to determine the value of the projectile shape coefficient. The projectile velocity was measured at 5.5 m and 12.2 m from the weapon muzzle. Corresponding values of the shape coefficient i were determined using Eq. (1) and the results are shown in Fig.7. One can easily see that the value of i is not constant; rather, it changes with velocity.

The measured mean impact velocities for each charge used, together with their confidence interval, and their approximations to the nearest tens are listed in Table 2. For convenience, these latter values will be used hereafter to refer to the values measured.

Figure 8 shows experimentally obtained residual projectile velocity V_r as function of impact velocity V_i for different plate thicknesses of as-received plates. It is clear that V_r increases with V_i in a quasi-linear fashion. Such results are in agreement with other investigations [4,9]. A linear regression analysis was performed and the best fit lines are also shown in the same figure. Figure 9 also shows experimentally obtained residual velocity as a function of V_i for different treated plate thicknesses, together with the best fit lines based on the least squares technique.

Figure 10 shows the change of projectile velocity drop ΔV versus the projectile impact velocity for the as-received plates. ΔV decreases and then increases again with the increase of V_i These results are consistent with other reports [9,10]. Ipson and Recht [9] interpreted such behaviour based on the application of momentum conservation principle. The impulse transferred to the target plate, and consequently the velocity drop decreases as V_i increases in the vicinity of the ballistic limit. For higher values of V_i , ΔV increases again as a result of changing of the plate deformation mechanism. Osborn and Maj [10] explained such behaviour by either thermal effects which lower the flow stress in the plastic range, or the effect of increasing the strain rate which will increase the initial yield stress of the material. Also, Fig.10 depicts the change of ΔV with the projectile impact velocity for treated target plates. The trend is similar to that of the as-received plates, but with different degree of non-linearity.

The projectile energy drop ΔE as a function of the impact velocity for different plate thickness is shown in Fig.11. It is clear that ΔE follows the same trend as that exhibited by the projectile velocity drop (cf. Fig.10), although with different degree of non-linearity. Figure 11 also presents the change of energy loss, ΔE, with V_i for treated duralumin plates. The curves show that the energy loss increases with impact velocity, alternatively with the deformation rate.

Figures 10 and 11 lead to the conclusion that increasing V_i does indeed increase the projectile ability to penetrate an armour of certain characteristics. At the same time, its residual velocity

increases, although ΔV and ΔE decrease. A critical impact velocity V_{ic} is eventually reached, beyond which both ΔV and ΔE begin to increase again. The values of projectile critical impact velocity are determined numerically employing the divided difference technique of the measurements, and the results are listed in Table 3.

The projectile velocity drop and energy loss during perforation of treated plates are greater than those of the as-received ones, although the yield and ultimate strengths of the treated plates are lower than the as-received plates. The reason of this is because the total strain to fracture is increased by treating and consequently the internal energy per unit volume, $U(=\int_0^{\epsilon_f} \sigma \, d\epsilon)$. As the energy lost during penetration is essentially consumed in overcoming the plate resistance, it becomes evident why the treated plates exhibited higher resistance to penetration. However, this conclusion is related to the particular mechanical properties of the plates and test conditions, and cannot be generalized.

Post-Firing Examination Results

Incomplete penetration was encountered at the velocities of 220 and 350 m/s for h_o = 4 mm (as-received and treated) and at 220 m/s for h_o = 3 mm (as-received only). The dominant failure mode in all cases of perforation was petalling, except for h_o = 3 mm (as-received) where plugging was exhibited at the particular impact velocity of 350 m/s. Examination of as-received plates showed that the number of petals ranged from five to six, while the separated cylindrical plugs were about 8.2 mm in diameter and 1.2 mm height. The projectile deformation increased by increasing the plate thickness. Some perforated hole diameters were measured, and their average values are listed in Table 4.

Figure 12 presents the results of penetration time measurements as a function of impact velocity. It is evident from the figure that the penetration time is linearly decreasing with the impact velocity. One has to note that the particular time measurement corresponding to V_i = 350 m/s and h_o = 3 mm is questionable; the plug, and not the perforating projectile had most likely activated the electronic counter.

PREDICTIONS AND COMPARISONS

The Ravid-Bodner model [5] was used to predict the main parameters associated with penetration of 3 mm as-received duralumin plate exhibiting plugging failure. Time histories of resisting force, velocity as well as travel advancement of projectile through target plate were obtained. Comparison between both experimental and predicted results was held.

The input data are projectile density, length, diameter and impact velocity, as well as target thickness, density and its material static flow stress. The values of impact velocity, static flow stress, and strain to fracture for the duralumin

plates were measured experimentally. The mean projectile density was calculated through the calculation of the projectile volume [10]. A material parameter needed to be evaluated for the plates material, and was found, by performing a sensitivity study, to be 0.175. Such parameter is used to express the dynamic flow stress in terms of static flow stress and effective strain rate.

Table 5 summarizes the predicted main penetration parameters associated with the process, together with some measured values. Moreover, Fig.13 shows the predicted time histories of the projectile displacement, velocity and resisting force for the 3 mm-thick as-received duralumin plates struck at V_i = 350 m/s. It is seen from this table that the experimental measurements and predicted values are in good agreement except for the time of penetration for the reason indicated earlier.

CONCLUSIONS

1. The projectile shape coefficient was found to change considerably with projectile velocity.
2. The change in projectile velocity drop and energy loss with impact velocity are qualitatively similar; they first decrease and then increase, which means that there is a critical impact velocity at which the projectile dissipated energy is minimum.
3. The total internal energy is the judge for increasing the penetration resistance of duralumin plates.
4. Comparison of main penetration parameters measured experimentally and those predicted using the Ravid-Bodner model shows a fairly good agreement.

REFERENCES

1. Riad,A.M., "Penetration of Thin Plates by Projectiles", M.Sc. Thesis, M.T.C., Cairo (1990).
2. Abdel-Kader,M.S., "The Penetration Capability of High Speed Projectiles Fired Against Brass and Steel Targets Plates",M.Sc. Thesis, M.T.C., Cairo (1981).
3. Backman,M.E. and Goldsmith,W., "The Mechanics of Penetration of Projectiles into Targets", Int.J. Engng. Sci., 16, 1-99 (1978).
4. Zukus,A., "Impact Dynamics", Wiely Interscience, New York, 157-210 (1982).
5. Ravid,M. and Bodner,S.R., "Dynamic Perforation of Visco-Plastic Plates by Projectiles", Int.J. Engng. Sci.,21, 577-591 (1983).
6. Anon, "External Ballistics", P.L No. 215, M.T.C., Cairo (1963).
7. Anon, "Internal Ballistics Measurements", P.L No. 1262, M.T.C, Cairo (1971).
8. Kupper,A., "Applied Regression Analysis and Other Multivariable Methods", Publishers, California (1978).
9. Ipson,T.W. and Recht,R.F., "Ballistic Perforation Resistance and Its Measurements", Exp. Mech., 15, 249-257 (1975).
10. Osborn,C.J. and Maj,S., "The Effect of Striking Velocity on Perforation Energy of Mild Steel Plates", Proc. Int. Conf. Fracture, 3, Pergamon Press, New York, 617-620 (1977).
11. Anon, "Ammunition Theory and Design", P.Ls. No. 15 and 21, M.T.C., Cairo (1959).

Table 1. Average Chemical Compostion of Duralumin in Wt. %.

Cu	Mg	Si	Fe	Mn	Ni	Zn	Pb	Ti	Cr	Al
4.51	0.65	0.19	0.31	0.77	0.02	0.1	0.01	0.01	0.01	Rem.

Table 2. Mean Impact Velocity and Their Approximate Confidence Interval for Different Charges.

Charge Mass, gm	Impact Velocity, m/s	Confidence Interval, m/s	Approximated Impact Vel., m/s
1.6	700.6	± 3.5	700
1.4	619.9	± 2.7	620
1.1	483.1	± 5.2	480
0.8	352.1	± 4.4	350
0.5	220.4	± 1.9	220

Table 3. Critical Impact Velocity, V_{ic} for Different Plate Thicknesses, h_o

h_o, mm	1.6	3.0	4.0
V_{ic}, m/s	425.23	580.45	585.37

Table 4. Perforated Hole Diameter Measurements for As-Received Plates at Different Impact Velocities.

h_o, mm	V_i, m/s 700	620	480
1.6	8.07	7.83	7.57
3.0	8.19	7.72	7.7
4.0	8.5	8.11	7.86

Table 5. Comparison of Predicted and Available Experimental Penetration Parameters for 3 mm As-Received Plates at V_i = 350 m/s.

Parameter	Prediction	Measurement
Plug velocity, m/s	296.7	---
Projectile exit velocity, m/s	245.1	235.5
Shear zone width, mm	4.9	---
Plug length, mm	1.6	1.2
Penetration time, μs	107.0	19.2
Projectile travel, mm	30.3	---
Maximum force, KN	64.2	---
Bulge height, mm	3.5	---
Bulge diameter, mm	8.5	---
Hole diameter, mm	8.46	8.2

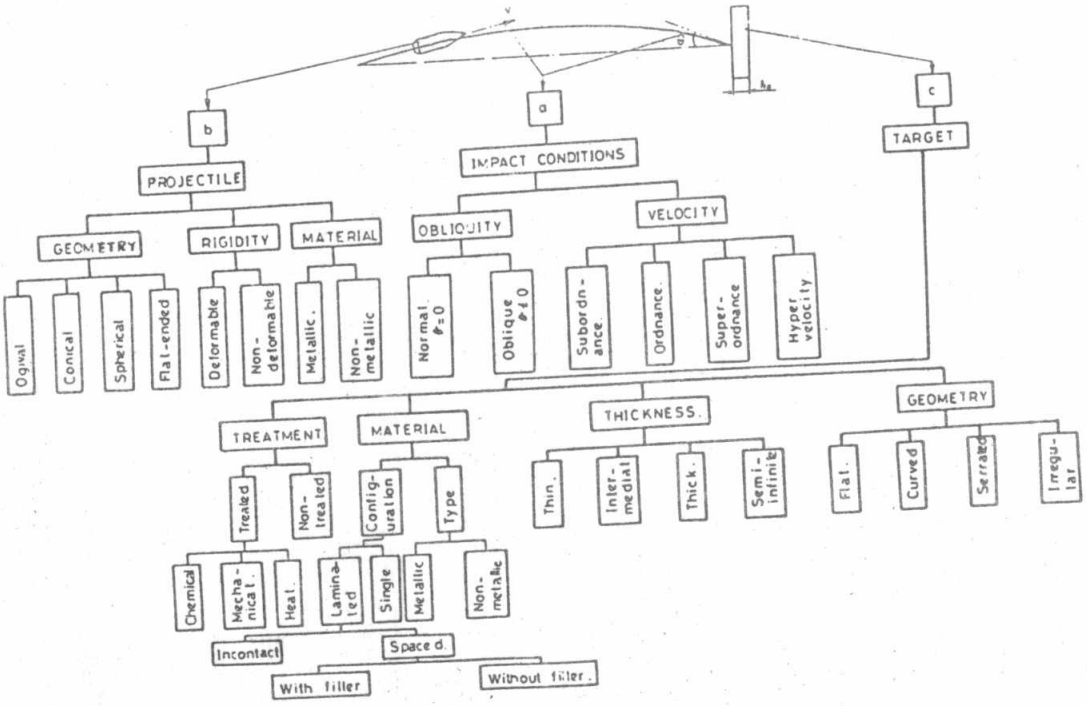

Fig. 1. Penetration parameters.

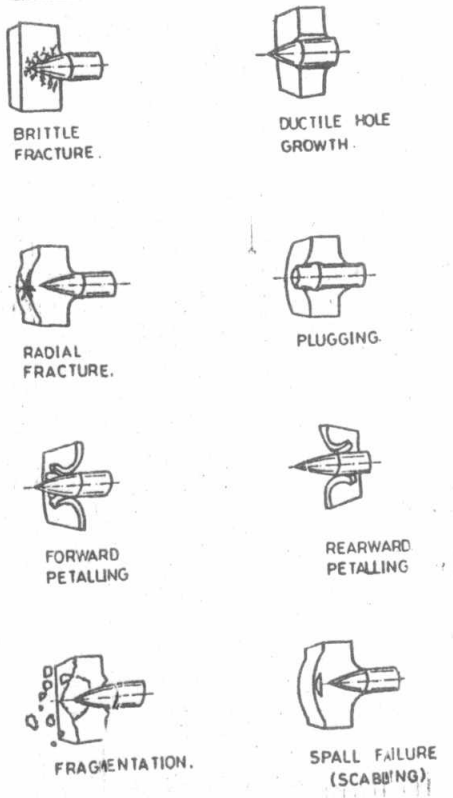

Fig. 2. Target failure mechanisms [3].

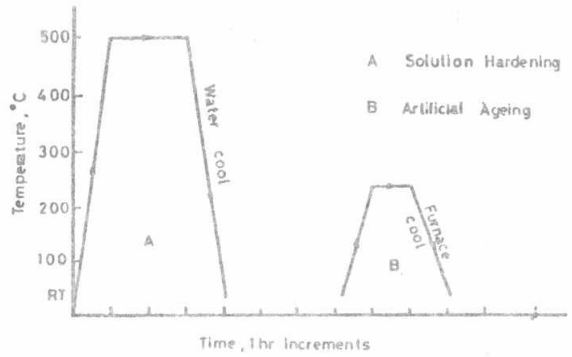

Fig. 3. Thermal cycle for duralumin plates.

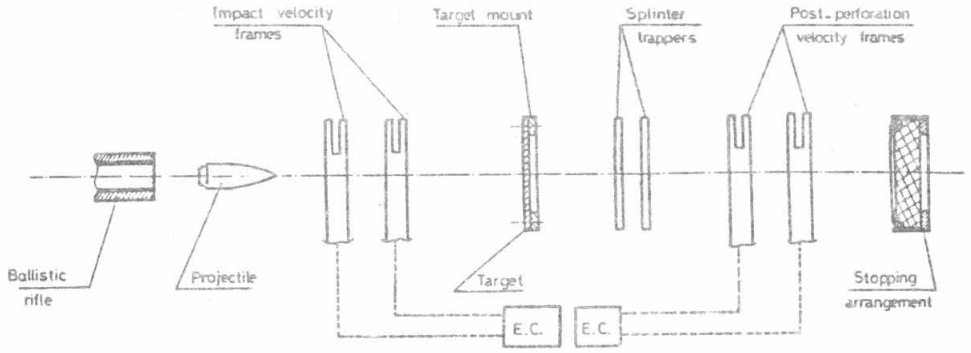

Fig. 4. Schematic of ballistic test arrangement.

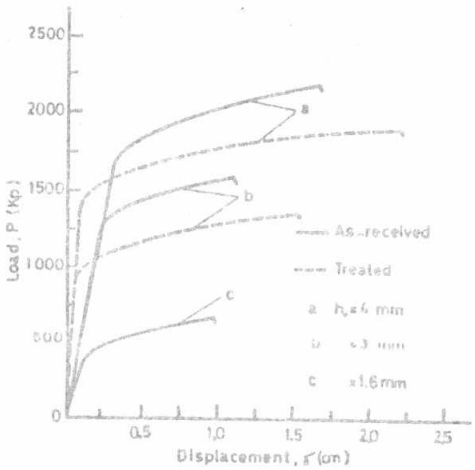

Fig. 5. Typical experimental load-displacement curves for as-received and treated duralumin plates.

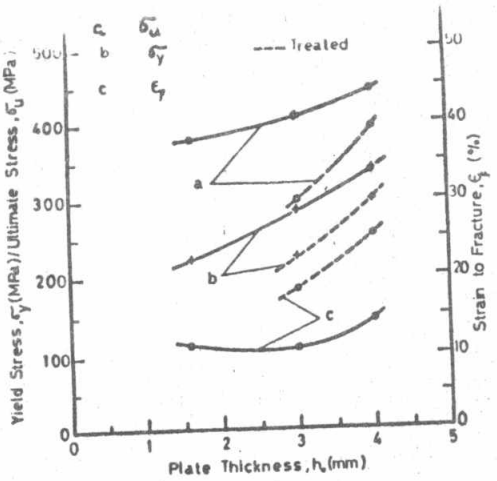

Fig. 6. Tensile test results of as-received and treated duralumin plates.

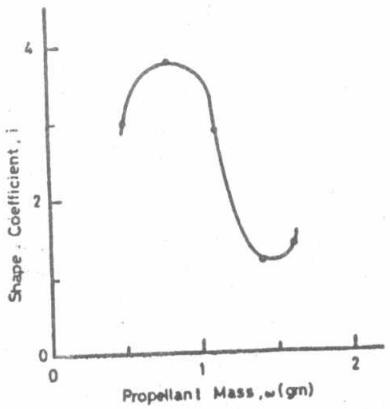

Fig. 7. Change of projectile shape coefficient with the propellant mass.

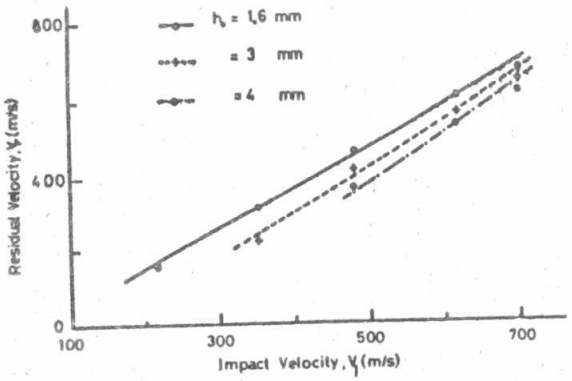

Fig. 8. Experimental and best straight line fit of V_r versus V_i for as-received duralumin plates.

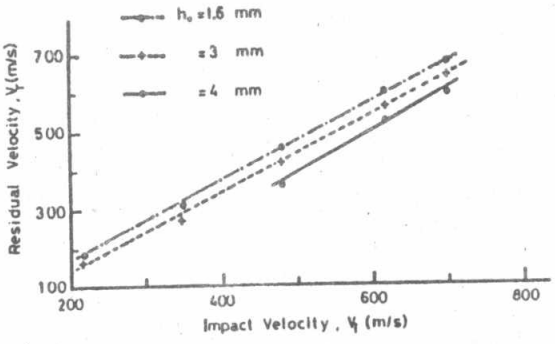

Fig. 9. Experimental and best straight line fit of V_r versus V_i for treated duralumin plates.

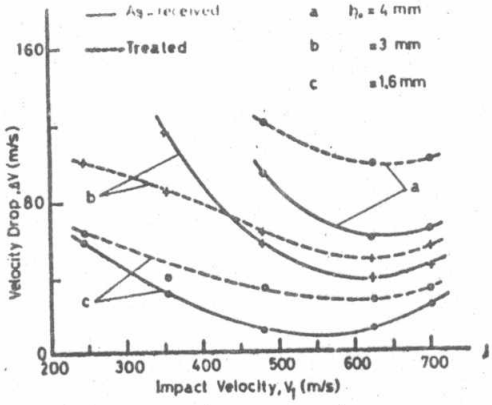

Fig. 10. Projectile velocity drop ΔV versus impact velocity V_i for as-received and treated duralumin plates.

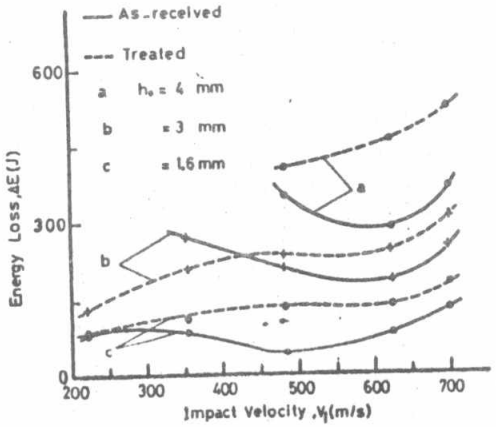

Fig. 11. projectile energy loss ΔE versus impact velocity V_i for as-received and treated duralumin plates.

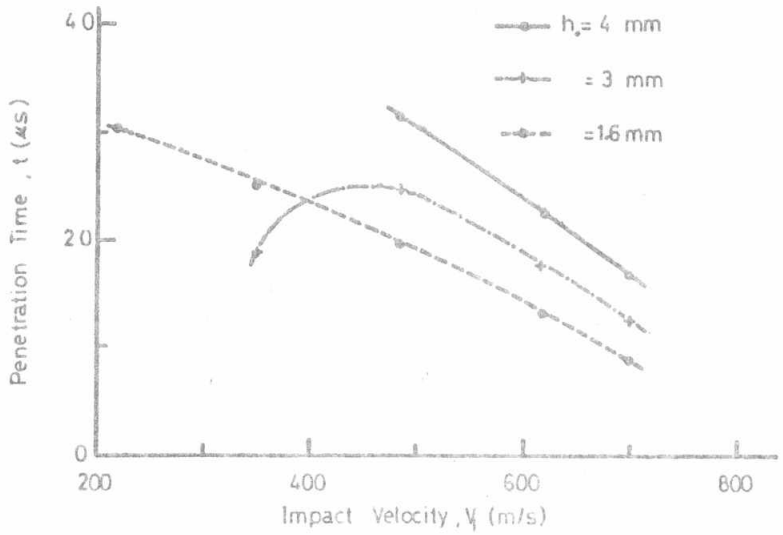

Fig. 12. Measured time of penetration versus projectile impact velocity.

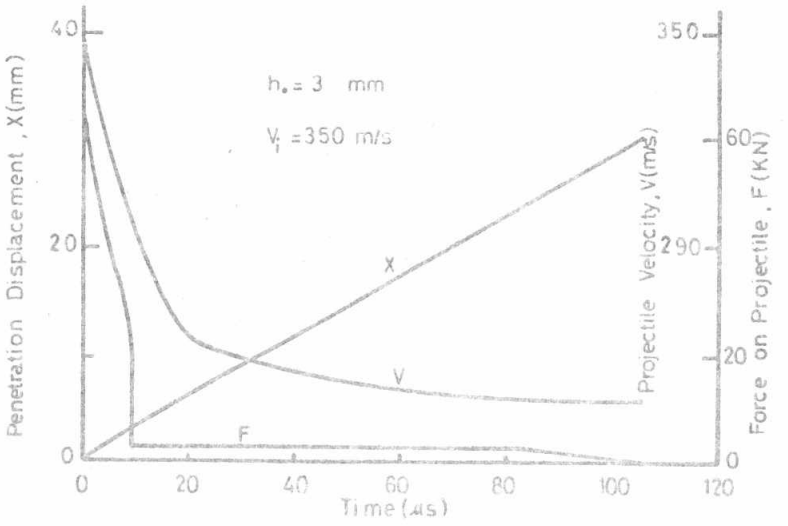

Fig. 13. Predicted time histories of projectile displacement, velocity and resisting force during perforation of 3 mm-thick, as-received duralumin plate at V_i =350 m/s.